Contribution from the Department of Chemistry,
North Carolina State University, Box 8204, Raleigh, North Carolina 27695-8204

X-ray Crystallographic Studies of Nickel(II) Complexes of Tetradentate $[N_2S_2]^{2-}$ Ligands. 3. A Stepwise Distortion from Square-Planar to Pseudotetrahedral Geometries

Eric M. Martin, Robert D. Bereman,* and Pirthu Singh

Received May 30, 1990

A series of neutral nickel(II) compounds of the tetradentate ligands *N,N'*-ethylene-, *N,N'*-trimethylene-, and *N,N'*-tetramethylenebis(methyl 2-amino-1-cyclopentenedithiocarboxylate) ($(CH_2)_n$ bridge: Ni $n = 2$, I; Ni $n = 3$, II; Ni $n = 4$, III) were prepared by reaction of the ligands with nickel acetate in methanol. The ligands differ only by the number of methylene groups, *n*, bridging the imine nitrogens of each half of the ligand. Trends in the physical characteristics of the complexes in solution suggested distortion from planar geometries and population of a triplet spin state. Crystals of each complex suitable for X-ray diffraction studies have been examined on a Nicolet R3m/μ diffractometer, thus allowing an analysis of the relationships between structure and spectral properties in a closely related series of NiN_2S_2 complexes. $NiC_{16}H_{22}N_2S_4 \cdot CH_2Cl_2$ (I) crystallizes in the space group $C2/c$ with $a = 31.18$ (1) Å, $b = 7.529$ (5) Å, $c = 26.78$ (1) Å, $\beta = 136.86$ (3)°, $V = 4298.5$ Å^3, and $Z = 8$. $NiC_{17}H_{24}N_2S_4$ (II) also crystallizes in the space group $C2/c$ with $a = 28.35$ (1) Å, $b = 9.015$ (5) Å, $c = 15.939$ (7) Å, $\beta = 107.47$ (4)°, $V = 3886.1$ Å^3, and $Z = 8$. $NiC_{18}H_{26}N_2S_4$ (III) crystallizes in the space group $P\bar{1}$ with $a = 8.230$ (3) Å, $b = 9.869$ (4) Å, $c = 13.460$ (4) Å, $\alpha = 105.87$ (3)°, $\beta = 95.04$ (3)°, $\gamma = 104.78$ (3)°, $V = 1002.0$ Å^3, and $Z = 2$. Block-diagonal least-square refinements of the trial structures result in discrepancy indices of $R = 4.53\%$, 4.32%, and 5.29%, respectively, for 1849, 2874, and 3500 used reflections. The NiSS' and NiNN' planes intersect to form dihedral angles of 3.4, 18.9, and 38.6°, for I, II, and III, respectively, displaying a systematic distortion from square-planar to pseudotetrahedral coordination geometry. Bond distances suggest thiolate-like S–Ni bonds and a large amount of electron delocalization in the π-system of the six-membered chelate rings. As the dihedral angle increases, the S–Ni bond lengths decrease, while the N–Ni bond lengths increase. ^{1}H and ^{13}C solution NMR studies, as well as solid-state ^{13}C CP/MAS NMR studies, indicate significant contact shifts of resonances, resulting from singlet–triplet ground-state equilibrium and extensive electron delocalization of odd spin into the HOMO. The possible relevance to N_2S_2 ligand systems of biological importance and their coordinating geometries is presented.

Introduction

There is great interest in distorted, four-coordinate $M^{II}N_2S_2$ complexes that may serve as spectral and geometrical mimics of metalloenzyme active sites found in nature. Fine tuning the electronic and magnetic properties of ligated metal ions has frequently involved varying not only the coordinating ligands but also the geometry of a constant set of donor atoms.[1] It is the magnitude of the geometrical influence that is often under consideration in dealing with structurally unresolved macromolecules in biological systems. Two metal systems that show extreme sensitivity to the influence of coordinating ligands are Ni(II) and Cu(II) four-coordinate compounds.[2-4]

The bioinorganic chemistry of nickel has become increasingly important in the past few years, primarily because of the presence of nickel at the active site of several very important classes of metalloenzymes, including the nickel hydrogenases and CO dehydrogenases,[5-7] but also because of the use of nickel(II) as a spectroscopic probe in metal replacement studies of other metalloenzyme systems.[8-12] Common to many investigations into nickel(II) metalloenzymes is the proposition of four-coordinate, distorted geometries involving nitrogen and sulfur ligand groups at the active sites. Examples include experiments using electron spin resonance, X-ray diffraction, and X-ray absorption techniques that suggest from one to four sulfurs bind a monomeric nickel ion at protein active sites.[13-17] Recent magnetic circular dichroism experiments have revealed the magnetic susceptibility of the nickel site in native hydrogenases is likely diamagnetic, suggesting planar coordination geometries.[18] Nickel(II) has been substituted into various type I Cu(II)-containing metalloenzymes where the metal is thought to be coordinated by two nitrogen and two sulfur groups. It has been shown that at least one Ni(II) derivative of a native Cu(II) enzyme absorbs radiation in the near-IR region,[11] characteristic of tetrahedral, or pseudotetrahedral, d^8 symmetries. Some information on $Ni(II)N_2S_2$ systems with tetradentate ligands has been collected;[19-34] however, a study of systematically varying

(1) Addison, A. W. *Inorg. Chim. Acta* **1989**, *162*, 217.
(2) Greenwood, N. N.; Earnshaw, A. *Chemistry of the Elements*; Pergamon Press: Oxford, England, 1980; p 1342.
(3) Greenwood, N. N.; Earnshaw, A. *Chemistry of the Elements*; Pergamon Press: Oxford, England, 1980; pp 1379–1386.
(4) Sacconi, L. *Transition Met. Chem. (N.Y.)* **1968**, *4*, 199.
(5) Hausinger, R. P. *Microbiol. Rev.* **1987**, *51*, 22.
(6) Cammack, R. *Adv. Inorg. Chem.* **1988**, *32*, 297.
(7) Lancaster, J., ed. *The Bioinorganic Chemistry of Nickel*; VCH Publishers, Inc.: New York, 1988.
(8) Cammack, R.; Patil, D. S.; Hatchikian, E. C.; Fernande, V. M. *Biochim. Biophys. Acta* **1987**, *98*, 912.
(9) Tennent, D. L.; McMillin, D. R. *J. Am. Chem. Soc.* **1979**, *101*, 2307.
(10) Lum, V.; Gray, H. B. *Isr. J. Chem.* **1981**, *21*, 23.
(11) Engeseth, H. R.; McMillin, D. R.; Ulrich, E. L. *Inorg. Chim. Acta* **1982**, *67*, 145.
(12) Blaszak, J. A.; Ulrich, E. L.; Markley, J. L.; McMillin, D. R. *Biochemistry* **1982**, *21*, 6253.
(13) DerVartanian, D. V.; Krüger, H.-J.; Peck, H. D., Jr.; LeGall, J. *Rev. Port. Quim.* **1975**, *27*, 70.
(14) Albracht, S. P. J.; Kroger, A.; Van der Zwaan, J. W.; Unden, G.; Bocher, R.; Mell, H.; Fontijn, R. D. *Biochim. Biophys. Acta* **1986**, *874*, 116.
(15) Lindahl, P. A.; Kojima, N.; Hausinger, R. P.; Fox, J. A.; Teo, B. K.; Walsh, C. T.; Orme-Johnson, W. H. *J. Am. Chem. Soc.* **1984**, *106*, 3062.
(16) Scott, R. A.; Wallin, S. A.; Czechowski, M.; DerVartanian, D. V.; LeGall, J.; Peck, H. D., Jr.; Moura, I. *J. Am. Chem. Soc.* **1984**, *106*, 6864.
(17) Cramer, S. P.; Eidsness, M. K.; Pan, W.-H.; Morton, T. A.; Ragsdale, S. W.; DerVartanian, D. V.; Ljundghal, L. G.; Scott, R. A. *Inorg. Chem.* **1987**, *26*, 2477.
(18) Kowal, A. T.; Zambrano, I. C.; Moura, I.; Moura, J. J. G.; LeGall, J.; Johnson, M. K. *Inorg. Chem.* **1988**, *27*, 1162.
(19) Lindoy, L. F.; Smith, R. J. *Inorg. Chem.* **1981**, *20*, 1314.
(20) Drummond, L. A.; Henrick, K.; Kangasundaram, M. J. L.; Lindoy, L. F.; McPartlin, M.; Tasker, P. A. *Inorg. Chem.* **1982**, *21*, 2963.
(21) Martin, J. W. L.; Organ, G. J.; Wainwright, K. P.; Weerasuria, K. D. V.; Willis, A. C.; Wild, S. B. *Inorg. Chem.* **1987**, *28*, 4531.
(22) Duckworth, P. A.; Stephens, F. S.; Wainwright, K. P.; Weerasuria, K. D. V.; Wild, S. B. *Inorg. Chem.* **1989**, *28*, 4531.
(23) Krüger, H.-J.; Holm, R. H. *Inorg. Chem.* **1988**, *27*, 3645.
(24) Ali, M. A.; Livingstone, S. E. *Coord. Chem. Rev.* **1974**, *13*, 101.
(25) Pangratz, W. R.; Urbach, F. L.; Blum, P. R.; Cummings, S. C. *Inorg. Nucl. Chem. Lett.* **1973**, *9*, 1141.
(26) Wei, R. M. C.; Cummings, S. C. *Inorg. Nucl. Chem. Lett.* **1973**, *9*, 43.
(27) Blum, P. R.; Wei, R. M. C.; Cummings, S. C. *Inorg. Chem.* **1974**, *13*, 450.
(28) Chen, L. S.; Cummings, S. C. *Inorg. Chem.* **1978**, *17*, 2358.
(29) Corrigan, M. F.; West, B. O. *Aust. J. Chem.* **1976**, *29*, 1413.
(30) Bertini, I.; Sacconi, L.; Speroni, G. P. *Inorg. Chem.* **1972**, *11*, 1323.
(31) Nag, K.; Joardar, D. S. *Inorg. Chim. Acta* **1975**, *14*, 433.
(32) Mondal, S. K.; Paul, P.; Roy, R.; Nag, K. *Transition Met. Chem. (Weinheim, Ger.)* **1984**, *9*, 247.
(33) Roy, R.; Paul, P.; Nag, K. *Transition Met. Chem. (Weinheim, Ger.)* **1984**, *9*, 152.
(34) Mondal, S. K.; Joardar, D. S.; Nag, K. *Inorg. Chem.* **1978**, *17*, 191.

0020-1669/91/1330-0957$02.50/0

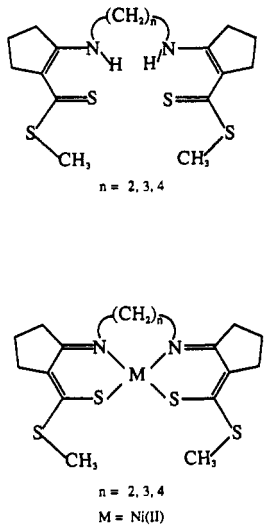

Figure 1. Lewis structures of Ni(II) complexes: $n = 2$ (I); $n = 3$ (II); and $n = 4$ (III).

stereochemistries has not been reported to our knowledge.

In an effort to better understand the relationship between tetrahedral distortion and spectral properties of four-coordinate Ni(II) complexes in general, we have designed a series of tetradentate $[N_2S_2]^{2-}$ ligands with flexibility that allows the attainment of both square-planar and pseudotetrahedral coordination geometries and have undertaken a detailed structural and stereoelectronic study of this series of soluble complexes.[35] The Lewis structures of the ligands and complexes are illustrated in Figure 1, where it is apparent that the complexes differ only by the number of methylene groups, n, bridging the "halves" of the ligands. The variation in geometry is achieved by increasing n, thereby causing distortion of the coordination geometry as the nitrogens continue to try to span cis positions around the central metal. Earlier, we reported the analogous Cu(II) series, where large distortions toward tetrahedral symmetry were found for both the Cu $n = 3$ and Cu $n = 4$ complexes.[36-38] We anticipated that the Ni(II) d^8 complexes would show less severe distortions and remain planar, gaining greater stabilization for the filled atomic orbitals.[2] Earlier reports indicated both $NiC_{16}H_{22}N_2S_4$ (I) and $NiC_{17}H_{24}N_2S_4$ (II) were planar.[33,34]

Preliminary studies on the solid-state properties of the Ni(II) complexes included characterization by ^{13}C cross-polarization magic-angle-spinning (CP/MAS) NMR spectroscopy. CP/MAS is now used routinely to obtain high-resolution spectra of solids, yet our understanding of the relationship between molecular structure and CP/MAS data remains somewhat limited.[39-44] One of the goals of our studies is to provide a comparison between data collected from solution ^{13}C NMR, solid-state ^{13}C CP/MAS NMR, and single-crystal X-ray analyses. In a series of four-coordinate NiN_2S_2 complexes where solution structures are thought to exist in a square-planar–tetrahedral geometrical equilibrium, a comparison between the solution and solid-state ^{13}C NMR spectra would allow more confident assignment of solution structures, especially where solid-state spectral data can be compared to refined molecular structures.

Table I. Crystallographic Data[a]

	I	II	III
chem formula	$C_{16}H_{22}N_2S_4Ni \cdot CH_2Cl_2$	$C_{17}H_{24}N_2S_4Ni$	$C_{18}H_{26}N_2S_4Ni$
fw	514.4	443.4	475.4
space group	$C2/c$	$C2/c$	$P\bar{1}$
T, K	296 (2)	296 (2)	296 (2)
I(Mo Kα), Å	0.71069	0.71069	0.71069
a, Å	31.18 (1)	28.35 (1)	8.230 (3)
b, Å	7.529 (5)	9.015 (5)	9.869 (4)
c, Å	26.78 (1)	15.939 (7)	13.460 (4)
α, deg	90.00	90.00	105.87 (3)
β, deg	136.86 (3)	107.47 (4)	95.04 (3)
γ, deg	90.00	90.00	104.78 (3)
V, Å^3	4298.5	3886.1	1002.0
Z	8	8	2
ρ(obsd), g/cm^3	1.60 (2)	1.50 (2)	1.50 (2)
ρ(calc), g/cm^3	1.59	1.52	1.52
μ, cm^{-1}	15.2	14.2	13.8
residuals, %	$R = 4.53$ $R_w = 6.37$	$R = 4.32$ $R_w = 6.33$	$R = 5.29$ $R_w = 7.26$

[a] $R = \sum||F_o| - |F_c||/\sum F_o$; $R_w = \{\sum w(\Delta F)^2/\sum F_o^2\}^{0.5}$; GOF $= \sum[w(|F_o| - |F_c|)^2/(N_o - N_v)]^{0.5}$.

Experimental Section

Materials. All reagents and solvents were commercially obtained from either Fisher Scientific or Aldrich Chemicals and used without further purification. Tetraalkylammonium salts, used as supporting electrolytes, were obtained from Southwestern Analytical Chemicals, dried for 12 h at 70 °C, and used without additional recrystallization. Aldrich Gold Label solvents were used for all electrochemical studies.

Syntheses. All compounds were prepared employing procedures previously reported.[31,35,45] Crystals of each compound were grown by slow evaporation from either $CHCl_3$ or CH_2Cl_2.

Physical Measurements. Electronic absorption spectra of methylene chloride solutions and diffuse mulls of Nujol oil were recorded on a Cary 2300 spectrophotometer over the UV–visible and near-infrared region. The data were collected and manipulated with an Apple IIe computer.

All elemental analyses were obtained from Atlantic Microlabs, Atlanta, GA, and were satisfactory.

Electrochemical properties were determined in solutions of dimethylformamide, with tetraalkylammonium perchlorate salts as supporting electrolytes, and with the use of conventional three-compartment "H" cells. A BAS CV 27 potentiostat and YEW Model 3022 A4 X-Y recorder were used in all cyclic voltammetry experiments. Measurements were made by using a platinum-disk working electrode and a platinum-wire auxiliary electrode, with potentials standardized against a saturated calomel electrode.

Solution ^1H and ^{13}C NMR spectra were obtained on either a GE 300-MHz Omega FT-NMR spectrometer, or a GE 500-MHz Omega FT-NMR spectrometer equipped with variable-temperature apparatus. All ^1H spectra were obtained by using $CDCl_3$ solutions with TMS as an internal standard. All solution ^{13}C spectra were standardized against the 77 ppm triplet of $CDCl_3$.

Solid-state ^{13}C CP/MAS spectra were recorded on either an IBM NR 100AF spectrometer at 25.18 MHz or a Chemagnetics 200S spectrometer at 50.14 MHz. The IBM instrument was equipped with a Doty probe. Compounds in their purified microcrystalline state were packed into a zirconia rotor with Kel-F Vespel end caps. The samples were oriented at 54° 44′ to the static field and spun at rates ranging from 2.5 to 3.5 kHz. Approximately 3000–5000 transients were collected for all samples over a spectral width of 15 kHz. All CP/MAS spectra were acquired with 2-ms contact (CP) times, 5-μs pulse widths, 3-s relaxation delay, and 2K data points. The signal to noise ratio for each spectrum was improved by apodization, which introduced 1-Hz line broadening. All shifts of solids were referenced to the upper most, 31 ppm, resonance observed in the spectrum of 1,4-di-*tert*-butylbenzene.

(35) Martin, E. M.; Bereman, R. D.; Dorfman, J. R. *Inorg. Chim. Acta*, in press.
(36) Bereman, R. D.; Dorfman, J. R.; Bordner, J.; Rilemma, D. P.; McCarthy, P.; Shields, G. D. *J. Bioinorg. Chem.* **1982**, 49.
(37) Bereman, R. D.; Churchill, M. W.; Shields, G. D. *Inorg. Chem.* **1979**, *18*, 3117.
(38) Bereman, R. D.; Shields, G. D.; Bordner, J.; Dorfman, J. R. *Inorg. Chem.* **1981**, *20*, 2165.
(39) Garroway, A. N.; Van der Hart, D. L.; Earl, W. L. *Philos. Trans. R. Soc. London, A* **1981**, *299*, 609.
(40) Balimann, G. E.; Groombridge, C. J.; Harris, R. K.; Packer, K. J.; Say, B. J.; Tanner, S. F. *Philos. Trans. R. Soc. London, A* **1981**, *299*, 643.
(41) Van der Hart, D. L.; Earl, W. L.; Garroway, A. N. *J. Magn. Reson.* **1981**, *44*, 361.
(42) Naito, A.; Ganapathy, S.; McDowell, C. A. *J. Chem. Phys.* **1981**, *74*, 5393.
(43) Sumner, S. C. J.; Moreland, C. G.; Carroll, F. I.; Brine, G. A.; Boldt, K. G. *Magn. Reson. Chem.* **1989**, *27*, 311.
(44) Kinoshita, S.; Wakita, H.; Yamashita, M. *J. Chem. Soc., Dalton Trans.* **1989**, 2457.
(45) Bordas, P.; Sohar, P.; Matolcsy, G.; Berencsi, P. *J. Org. Chem.* **1972**, *37*, 1727.

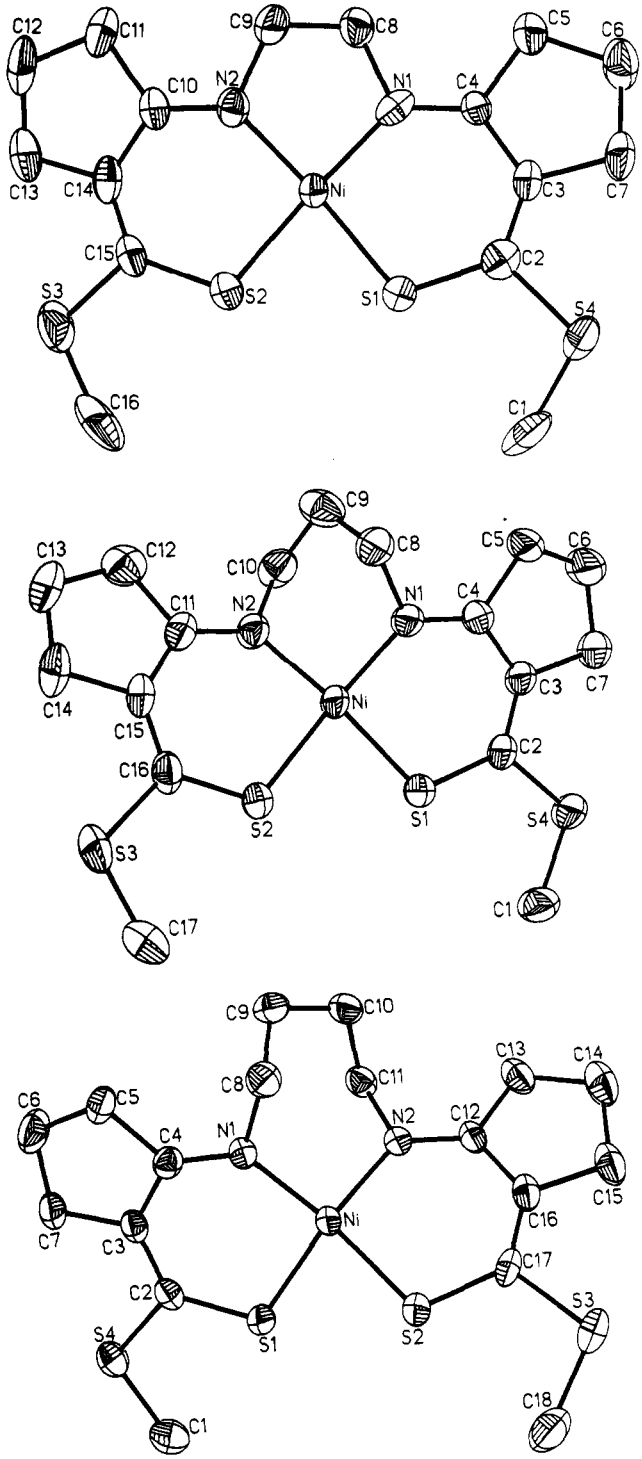

Figure 2. Thermal ellipsoid plots showing molecular structure: (a, top) Ni $n = 2$ (I); (b, middle) Ni $n = 3$ (II); (c, bottom) Ni $n = 4$ (III).

Single-crystal X-ray analyses were collected on a Nicolet R3m/μ diffractometer comprising a four-circle Eulerian cradle goniometer, graphite monochromator, molybdenum radiation source ($\lambda = 0.71069$ Å operating at 48 kV and 26 MA), and dedicated Data General Microeclipse microprocessor.

Results and Discussion

Structure Solution and Refinement. All pertinent crystallographic data are displayed in Table I. Representative crystals of each compound were selected, mounted on a goniometer head, and surveyed. Cell dimensions were obtained by least-squares fits of 15 setting angles of the appropriate high-angle reflections. Data were corrected for Lorentz and polarization effects, but not for absorption, owing to the low absorption coefficients calculated for each of the crystals.

Table II. Selected Bond Distances (Å) for I, II, and III

	I	II	III
Ni-S1	2.174 (4)	2.160 (1)	2.162 (1)
Ni-N1	1.893 (6)	1.910 (2)	1.919 (4)
Ni-S2	2.170 (2)	2.173 (1)	2.161 (1)
Ni-N2	1.902 (11)	1.916 (3)	1.923 (3)
S1-C2	1.730 (12)	1.716 (3)	1.716 (4)
C2-C3	1.351 (9)	1.358 (5)	1.363 (6)
C3-C4	1.439 (18)	1.428 (5)	1.440 (5)
C4-N1	1.312 (17)	1.305 (4)	1.311 (5)
S4-C2	1.776 (15)	1.760 (4)	1.763 (4)
S4-C1	1.767 (7)	1.801 (4)	1.789 (6)
N1-C8	1.469 (16)	1.486 (4)	1.491 (5)
C8-C9	1.467 (17)	1.513 (6)	1.534 (5)
C9-C10		1.527 (5)	1.521 (7)
C3-C7	1.507 (16)	1.520 (5)	1.505 (6)
C7-C6	1.510 (12)	1.522 (6)	1.522 (8)
C6-C5	1.524 (40)	1.521 (6)	1.506 (7)
C4-C5	1.488 (8)	1.512 (5)	1.511 (7)

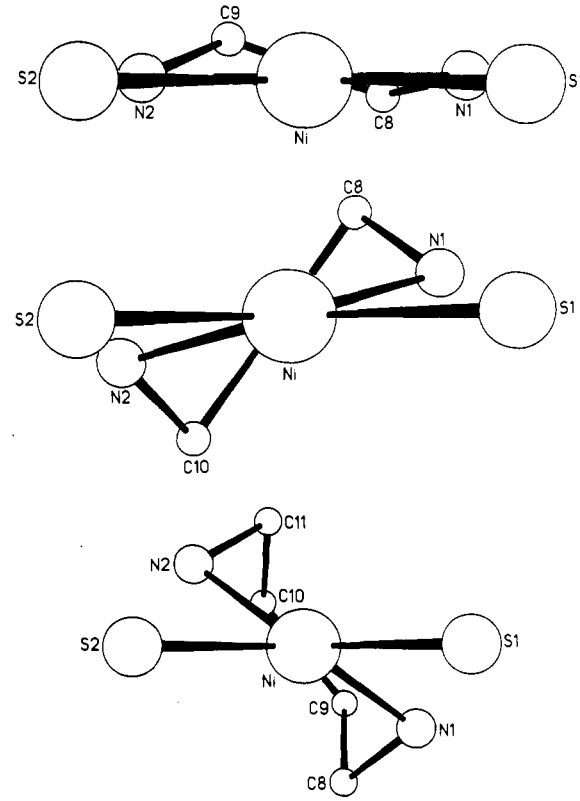

Figure 3. Views showing the distortion of the inner coordination sphere: (a, top) Ni(II) $n = 2$ (I); (b, middle) Ni(II) $n = 3$ (II); (c, bottom) Ni(II) $n = 4$ (III).

Nickel and sulfur atoms were located by direct methods using the crystallographic software packages SHELXTL provided by Nicolet.[46] The remaining non-hydrogen atoms were found by conventional difference Fourier techniques to give the appropriate trial structures. The structures were further refined by the block-diagonal least-squares technique using SHELXTL. The non-hydrogen atoms were refined with anisotropic temperature factors, while all hydrogen atoms were placed in calculated positions 0.96 Å away from attached carbon nuclei and not refined. Atomic scattering factors for all atoms were taken from ref 47. Final R indices are provided in Table I. Final difference Fourier maps revealed no missing or misplaced electron density. The refined structures were plotted with the SHELXTL graphics package. Hydrogen coordinates, bond distances and angles, anisotropic temperature factors, and calculated and observed structure factors

(46) Sheldrick, G. M. *SHELXTL*; X-ray Instruments Group, Nicolet Instrument Corp.: Madison, WI, 1985.
(47) *International Tables for X-Ray Crystallography*; Kynoch: Birmingham, England, 1974; Vol. IV, pp 71-102.

Table III. Selected Bond Angles (deg) for I, II, and III

	I	II	III
N1-Ni-S1	96.5 (4)	95.3 (1)	96.9 (1)
N2-Ni-S2	95.3 (2)	93.9 (1)	97.2 (1)
S1-Ni-S2	80.5 (1)	81.9 (1)	81.9 (1)
N1-Ni-N2	87.7 (4)	90.6 (1)	95.1 (1)
Ni-N1-C8	111.1 (8)	112.7 (2)	114.1 (3)
Ni-S1-C2	110.2 (1)	110.0 (1)	110.5 (4)
N1-C4-C3	125.9 (6)	126.8 (3)	126.9 (4)
S1-C2-C3	127.1 (12)	126.4 (3)	127.2 (3)
C2-C3-C4	126.6 (12)	125.8 (3)	125.6 (4)
S1-C2-S4	116.8 (4)	118.8 (3)	117.5 (2)

are available as supplemental material.

Selected bond distances and angles for the three compounds are reported in Tables II and III. Atom coordinates are given in Table IV. Figure 2 offers views of molecules I, II, and III, and Figure 3 provides a view of the inner coordination geometry and the diimine bridging backbones, where the distortion is most evident.

$C_{16}H_{22}N_2S_4Ni\cdot CCl_2H_2$ (I). Green prismatic crystals suitable for X-ray analysis were grown by the slow evaporation of a methylene chloride solution. A needle 0.4 × 0.1 × 0.1 mm was sealed in a capillary tube and mounted on the goniostat, and a data set was collected. Unit cell constants and axial photographs revealed the crystal possessed monoclinic symmetry. The systematic absences were consistent with the space group *Cc* or *C2/c*; the latter was confirmed by the successful refinement of the structure. Two check reflections every 98 scans indicated mean decomposition by 13% during the collection period. Further difference Fourier maps revealed the presence of one methylene chloride solvent molecule per molecule of nickel(II) complex. Decomposition of the crystal framework is attributed to the slow evaporation of solvent molecules from the lattice. Of 2632 unique reflections recorded in the range $3° \le 2\theta \le 44°$, 1849 with $I \ge 1.5\sigma(I)$ were used in the refinement of the final structure. The quantity minimized during the least-squares refinement was $\sum w(\Delta F)^2$, where $w^{-1} = \sigma_{F^2} + 0.00040(F)^2$.

$C_{17}H_{24}N_2S_4Ni$ (II). A reddish brown crystal with dimensions 0.3 × 0.2 × 0.2 mm was used in the X-ray diffraction study of II. Axial photographs and systematic absences again demonstrated that the crystal possessed monoclinic symmetry and belonged to the space group *Cc* or *C2/c*; the latter was again confirmed by successful refinement of the trial structure. No unexpected variations in intensities were observed in check reflections recorded every 98 measurements. A total of 3439 unique reflections were recorded within the range $3° \le 2\theta \le 50°$. Of those, 2874 measurements with $I \ge 4\sigma(I)$ were used in the refinement of the final structure. The quantity minimized during the least-squares refinement was $\sum w(\Delta F)^2$, where $w = \sigma_{F^2} + 0.00060(F)^2$.

$C_{18}H_{26}N_2S_4Ni$ (III). Reddish brown crystals of III were grown by slow evaporation of a saturated methylene chloride solution. A crystal with dimensions 0.5 × 0.4 × 0.2 mm was mounted and a data set collected. Out of 4617 unique reflections gathered within the range $3° \le 2\theta \le 55°$, 3500 with $I \ge 3\sigma(I)$ were used in the analysis. The crystal belonged to the primitive space group $P\bar{1}$. Check reflections every 98 scans indicated no unexpected variations in intensities. The quantity minimized during the least-squares refinement was $\sum w(\Delta F)^2$, where $w = \sigma_{F^2} + 0.00180(F)^2$.

Table IV. Atomic Coordinates (×10⁴) and Isotropic Thermal Parameters (Å² × 10³) for Complexes I, II, and III (Ni *n* = 2, *n* = 3, and *n* = 4)

	x	*y*	*z*	*U*[a]		*x*	*y*	*z*	*U*[a]
				Complex I					
Ni	2912 (1)	748 (2)	1525 (1)	30 (1)	C6	1798 (4)	−617 (4)	−1170 (4)	54 (8)
S1	3649 (1)	576 (4)	1593 (1)	43 (2)	C7	2484 (4)	−137 (12)	−630 (4)	47 (9)
S2	3718 (1)	1353 (4)	2675 (1)	49 (2)	C8	1649 (4)	3 (12)	295 (4)	42 (7)
N1	2235 (3)	253 (9)	514 (4)	36 (6)	C9	1682 (4)	1040 (14)	786 (4)	47 (8)
N2	2313 (3)	939 (9)	1541 (3)	35 (6)	C10	2367 (4)	1068 (11)	2071 (4)	34 (7)
S3	4128 (1)	1505 (4)	4090 (1)	66 (2)	C11	1813 (4)	1155 (14)	1955 (4)	53 (9)
S4	3861 (1)	395 (4)	672 (1)	55 (2)	C12	2104 (4)	1129 (14)	2716 (4)	64 (11)
C1	4616 (4)	668 (20)	1575 (5)	84 (11)	C13	2807 (4)	1109 (14)	3268 (4)	58 (9)
C2	3329 (4)	356 (11)	731 (4)	38 (3)	C14	2949 (4)	1093 (12)	2840 (4)	38 (8)
C3	2720 (4)	84 (11)	97 (4)	31 (7)	C15	3524 (4)	1268 (11)	3131 (4)	36 (7)
C4	2202 (4)	12 (11)	2 (4)	31 (6)	C16	4827 (4)	1763 (16)	4337 (4)	81 (9)
C5	1617 (4)	−379 (13)	−778 (4)	45 (8)					
				Complex II					
Ni	1220 (1)	5786 (1)	9643 (1)	34 (1)	C6	2126 (2)	10966 (4)	10176 (3)	65 (2)
S1	1539 (1)	6053 (1)	8580 (1)	51 (1)	C7	2156 (2)	10223 (4)	9337 (2)	55 (1)
S2	914 (1)	3802 (1)	8905 (1)	50 (1)	C8	1640 (1)	7154 (4)	11304 (2)	48 (1)
N1	1599 (1)	7327 (3)	10358 (2)	37 (1)	C9	1167 (1)	7600 (4)	11492 (2)	55 (1)
N2	816 (1)	5631 (3)	10412 (2)	39 (1)	C10	719 (1)	7092 (4)	10746 (2)	51 (1)
S3	618 (1)	749 (1)	9266 (1)	73 (1)	C11	639 (1)	4459 (4)	10689 (2)	39 (1)
S4	1979 (1)	8400 (1)	7718 (1)	54 (1)	C12	394 (1)	4439 (4)	11404 (2)	55 (1)
C1	1899 (2)	6827 (4)	6992 (2)	57 (2)	C13	313 (2)	2849 (5)	11573 (3)	86 (2)
C2	1798 (1)	7783 (4)	8622 (2)	39 (1)	C14	489 (2)	1891 (4)	10948 (3)	61 (2)
C3	1886 (1)	8756 (4)	9302 (2)	40 (1)	C15	654 (1)	2975 (4)	10369 (2)	43 (1)
C4	1821 (1)	8469 (3)	10141 (2)	39 (1)	C16	731 (1)	2615 (4)	9586 (2)	44 (1)
C5	2059 (2)	9706 (4)	10765 (2)	53 (1)	C17	735 (2)	587 (5)	8242 (3)	78 (2)
				Complex III					
Ni	7292 (1)	4475 (1)	7328 (1)	27 (1)	C7	7976 (5)	4980 (4)	3850 (3)	37 (1)
S1	7140 (1)	2620 (1)	5982 (1)	37 (1)	C8	6638 (5)	7131 (4)	7156 (3)	37 (1)
S2	6171 (2)	2737 (1)	7966 (1)	41 (1)	C9	8117 (6)	8548 (4)	7634 (3)	42 (2)
N1	7193 (4)	5855 (3)	6575 (2)	28 (1)	C10	9171 (6)	8572 (4)	8629 (3)	41 (1)
N2	8409 (4)	5949 (3)	8637 (2)	29 (1)	C11	9744 (5)	7207 (4)	8528 (3)	36 (1)
S3	5174 (2)	2241 (1)	9938 (1)	50 (1)	C12	8306 (5)	5926 (4)	9603 (3)	30 (1)
S4	7836 (2)	1923 (1)	3796 (1)	47 (1)	C13	9387 (6)	7101 (5)	10570 (3)	44 (2)
C1	7596 (9)	253 (5)	4126 (4)	64 (2)	C14	8576 (7)	6814 (6)	11489 (3)	59 (2)
C2	7564 (5)	3212 (4)	4920 (3)	31 (1)	C15	7365 (7)	5248 (5)	11100 (3)	47 (2)
C3	7695 (5)	4579 (4)	4836 (3)	30 (1)	C16	7198 (5)	4793 (4)	9921 (3)	34 (1)
C4	7351 (4)	5767 (4)	5601 (3)	30 (1)	C17	6287 (5)	3433 (4)	9289 (3)	33 (1)
C5	7128 (6)	6891 (5)	5072 (3)	41 (2)	C18	4183 (7)	543 (5)	8923 (4)	60 (2)
C6	7798 (7)	6526 (6)	4057 (4)	54 (2)					

[a] Equivalent isotropic *U* defined as one-third of the trace of the orthogonalized U_{ij} tensor.

Table V. Structure Property Relationships for I, II, and III

	dihedral angle, deg	electronic transitions, 10^3 cm^{-1} CH_2Cl_2 LF	CH_2Cl_2 LMCT	Nujol LF	Nujol LMCT	E, V $E_{1/2,ox}$	E, V $E_{1/2,red}$	$\delta(^1H)$, ppm 5-CH_2	$\delta(^1H)$, ppm 7-CH_2
Ni n = 2, I	3.4	15.2	22.6	15.1	22.0	0.75	−1.54	2.620	2.560
Ni n = 3, II	18.9	14.9	22.1	15.0	21.9	0.68	−1.43	2.515	2.617
Ni n = 4, III	38.6	14.8	21.8	14.6	20.8	0.59	−1.27	2.144	3.142

Description of Structure. The structure of each of the NiN_2S_2 complexes consists of discrete well-separated monomers with inner coordination spheres that distort from planar to pseudotetrahedral geometries in the order I, II, and III. Though I and II both crystallize in the monoclinic $C2/c$ space group, both contain one molecule in the asymmetric unit, thereby disallowing rigid crystallographic C_2 symmetry within each molecule. Thermal ellipsoid plots displaying the molecular structures and atom labels are shown in Figure 2, with a better representation of the inner coordination spheres shown in Figure 3. Views in Figure 3 are directed along the NiSS′ plane, with the nitrogens and methylene bridge located behind the Ni atom in each drawing. Table II lists some selected bond angles and distances for the compounds in the series. The dihedral angles as measured by the intersection of the NiNN′ and NiSS′ planes are 3.4, 18.9, and 38.6°, for I, II, and III, respectively. An angle of zero would of course indicate a planar structure, while a 90° dihedral angle would signify a tetrahedral coordination environment. The systematic rotation of the nitrogens out of the NiSS′ plane is very evident from Figure 3.

It is apparent from the bond lengths within the six-membered chelate rings of each of the complexes that the actual electronic structures of I, II, and III differ from the Lewis structures of the free ligands.[35] The formal double bonds should now be drawn between N1–C4 and C2–C3, indicating a Schiff base type coordinating ligand with an iminate nitrogen and pseudothiolate sulfur. A chelating ligand system of this type fits in well with the observed spectroscopic results.

The metal–ligand bond lengths are also interesting because few neutral, tetrahedrally distorted $Ni^{II}N_2S_2$ complexes have been studied crystallographically. Statistically significant bond distance changes are seen in the Ni–N and Ni–S bond distances in going from I to III. The Ni–S distances become shorter as the tetrahedral distortion increases, while the Ni–N bonds increase in length. Alternatively, intraligand strain may account for some portion of the bond distance changes. This trend in bond lengths is also seen in the Cu(II) complexes of this series of ligands and does not support an earlier proposal that bond distances inevitably increase when changing from square-planar to tetrahedral coordination geometries that involved identical sets of ligands or donor atoms.[4] With Ni–N distances of 1.91 Å and Ni–S distances of 2.16 Å, however, the bond lengths do not differ significantly from previously reported values for four-coordinate NiN_2S_2 complexes.[4]

Noteworthy in the case of II is the inequality between each half of the ligand. Both sets of Ni–N and Ni–S bond distances differ by 0.010 (1) Å, resulting in half of the ligand being apparently more tightly bound. The 18.9° distortion of the inner coordination sphere may not be sufficient to allow both S atoms access to equivalent $d\pi$ orbitals of metal origin. Thus, by increasing the distortion from 3.4° in I to 18.9° in II, one Ni–S bond becomes shorter and one Ni–N bond becomes longer. By going from 18.9° in II to 38.6° in III, the second set of Ni–S and Ni–N adjusts in similar fashion. In order to aid the following explanation, we have adopted a convention for a Cartesian coordinate system that utilizes Ni as the origin and labels the z axis as perpendicular to the NiSS′ plane. Accordingly, the x and y axes must each extend toward one of the bound sulfur atoms. In a square-planar molecule with a d^8 metal ion and two sulfurs and two nitrogens aligned trans to one another, all the chelating atoms must compete for the empty metal $d_{x^2-y^2}$ orbital. Without a bridging group and steric hindrance at the N positions the trans-planar configuration is stabilized.[48]

(48) Unpublished results.

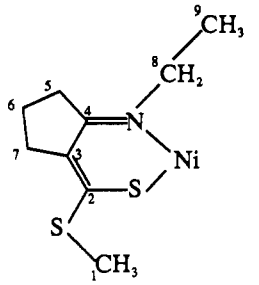

Figure 4. Labeling scheme used for assigning ^{13}C NMR resonances of I–III.

By effecting slight changes in ligand structure, we have "trapped" geometries in between these two cases. As the length of the diimine bridge increases, the nitrogens are forced out of the xy plane, allowing for increased covalency in the Ni–S bonds. The importance of molecular stereochemistry in relation to covalency of the M(II)–S bond is therefore seen as crucial and is affected by even subtle geometrical changes. Compound II represents a complex with symmetrical bonding groups, yet unsymmetrical bonds.

Spectral Characteristics. Table V provides a comparison of dihedral angles, LF transitions, LMCT transitions, $E_{1/2,ox}$ and $E_{1/2,red}$ values, and 5-C and 7-C ^1H NMR resonances for the three compounds. A plot of dihedral angles versus any one of these spectral features yields a straight line, suggesting a direct relationship between the physical properties and inner coordination sphere stereochemistry. Increased bonding interaction between the "soft" S atoms and Ni(II) has a significant effect on the trends in spectroscopic values. Again, by defining a coordinate system with the z axis perpendicular to the mean plane of the nickel and coordinating sulfur atoms, we reason that rotating the σ-donating nitrogens toward the z axis and moving the two π-donating sulfur donor atoms closer to the central metal along the x and y axes stabilize the metal-based $d_{x^2-y^2}$ orbital and destabilize the filled d_{xy} atomic orbital. Support for this hypothesis comes from spectroscopic results. Going from I to III, we observe that the complexes are both more easily oxidized and more easily reduced according to data from cyclic voltammetry experiments. Analysis of integrated peak intensities ($i_{p,c}/i_{p,a}$ = 1) and peak to peak separations (δE = 65 mV) at various scan rates confirm a one-electron reversible reduction. One-electron oxidations grow increasingly less reversible based on δE values beginning with I (70 mV) and proceeding to III (120 mV).

The subsequent increased delocalization within the chelate ring can be traced by examining the changes in bond lengths and angles, and by NMR spectroscopy. Table VI offers a summary of all the ^{13}C NMR data. Solution ^{13}C NMR data for both the ligands and complexes, and solid-state ^{13}C data for the complexes are tabulated. Although both "halves" of the ligand are crystallographically inequivalent, the carbon positions given in Table VI refer to the numbering scheme given in Figure 4. Doublets of equal intensity are indicated by two resonances and explained by the crystallographic differences. Exceptions are seen in the cases of positions C-8 and C-3, where dipolar interaction from neighboring nitrogens has been established by independent experiments at 25 and 50 MHz. The high value for the resonance from the carbons at the C-8 position in I can be attributed to the summation of effects from a nitrogen both α and β to the respective carbon. Theoretically, a crossover point exists between the ground-state singlet and the ground-state triplet of the pure D_{4h} and T_d symmetries. To monitor the spin-state mixing and predict

Table VI. ^{13}C NMR Chemical Shift Data for Free LIgands (L) and Ni(II) Complexes (Ni) I, II, and III as $CDCl_3$ Solutions and as Solids

	chem shift, ppm								
	I			II			III		
	soln		solid	soln		solid	soln		solid
carbon positions	L	Ni	Ni	L	Ni	Ni	L	Ni	Ni
1	17.31	16.97 16.09	17.29	17.30	16.91	15.61	17.27	19.12	16.29 18.03
2	199.71	172.74	173.36	199.81	173.74	174.53 175.17	197.97	171.77	174.75
3	119.23	124.56	123.93 123.52	119.14	125.60	123.96 125.53	119.04	128.51	123.67
4	169.25	157.45	155.28	169.57	156.65	151.17 153.27	169.51	147.77	151.18 150.50
5	34.19	36.88	36.08 39.97	34.16	35.84	34.52 36.31	34.03	39.40	34.97
6	21.30	22.21	23.47	30.25	27.15	26.93	27.90	31.68	28.63
7	33.51	33.06 33.00	33.01 34.47	33.58	32.42	32.69	32.52	32.00	32.74
8	54.67	57.20	56.40 60.25	45.44	48.64	46.21 48.30	45.44	59.91	58.46 61.75
9				21.30	22.50	21.72	21.30	22.47	21.73

the solution-state stereochemistry, both solution ^1H and ^{13}C and solid-state ^{13}C NMR studies were undertaken. Variable-temperature isotropic ^1H NMR spectroscopy revealed that only III exhibited significant contact shifts within the range of temperatures studied.[35] Assuming contributions from only paramagnetic contact interactions, we estimated the proportion of tetrahedral molecules at approximately 2–3%. The pairing energy is no longer significantly larger than the crystal field stabilization energy gained from filling the metal based d_{xy} orbital; thus, about 2–3% of complex III exists in the nondegenerate $(d_{xy})^1$ $(d_{x^2-y^2})^1$ configuration at room temperature, forming a triplet ground state. It will be interesting to see whether further distortion of the coordination environment involves additional small changes in dihedral angle and persistent triplet configuration or whether a dihedral angle of 90° can be obtained and a tetrahedral coordination environment stabilized.

Solution ^{13}C spectra of the free ligands were readily interpreted from literature collections of ^{13}C NMR shifts. Magnetic equivalence between the "halves" of each ligand results from similar structure and rotational averaging. Equivalence was also noted in spectra of the chelated ligands. Assignments of carbon shifts in the complexes were made with the aid of previous knowledge of spin densities obtained in the treatment of isotropic contact shifts of ^1H resonances and through interpretation of ^{13}C dipolar splitting constants arising at C-3 and C-8 at both 25 and 50 MHz. The higher field resonance reported for both of these positions represents the broadened shoulder characteristic of splitting from a neighboring nitrogen. At higher field the asymmetric doublets coalesced. Shifts in the ^{13}C resonances of the coordinated ligands result from a ligand to metal antiparallel spin transfer that polarizes the HOMO on the ligand, as reported earlier.[35,49-51]

Because a relaxation of the distorted geometries discovered in the solid state may occur in solution, ^{13}C NMR spectra were obtained on the crystalline complexes and their solutions. Initial indications, based on interpretation of the solution and Nujol mull electronic absorption results, indicated slight differences exist in the solution and solid-state structures of the Ni(II) complexes. Solid-state CP/MAS ^{13}C NMR data obtained on both the free ligands and complexes showed some similarity to solution spectra, however significant differences manifested at the C-8 positions. Similar solid-state and solution ^{13}C NMR spectral data would mandate similar structures in the two states. Correlations with the molecular structures of the three complexes confirmed that even small crystallographic differences between the halves of the chelated ligands could be resolved by the ^{13}C CP/MAS NMR technique employing 25- and 50-MHz frequency spectrometers. The results support previous assignments of flattened, more planar solution geometries predicted by interpretation of optical absorption and electrochemical data; however, they suggest that in solution the complexes exist in more tetrahedrally distorted coordination geometries.

The trend in dihedral angles for the Ni(II) complexes is remarkably stepwise, increasing by about 18° with each methylene group addition. This is in stark contrast to the corresponding Cu(II) series of the same ligands.[36-38] In the Cu(II) series, the dihedral angle rises abruptly from 20.0 to 53.9° for the transition from Cu $n = 2$ to Cu $n = 3$ and then nearly levels off, only increasing to 57.1° for Cu $n = 4$. This trend suggests that the Cu(II) ion prefers the more pseudotetrahedral geometry, but is limited by the alkyl chain length in the diimine bridge, while Ni(II) seems to remain most stable in the square-planar geometry. Thus, the ligand system forces the stereochemical changes that allow for greater covalency in the two Ni–S bonds.

It is also noteworthy to point out that a change in dihedral angle of ~15° causes a color change in the Ni(II) complexes from green to red. The predominant change in molecular structure involved in this color change appears to be the 0.010 (2) Å change in one Ni–S bond length.

The results are encouraging in that it is evident that only small geometric or electronic changes can produce significant changes in physical properties. Perhaps lower redox potentials for Ni(II)/Ni(III) couples in synthetic complexes can be obtained by placing nickel(II) in an anionic, distorted tetrahedral, or high-spin square-planar environment. The Ni–S and Ni–N bond lengths in I, II, and III are comparable to the two Ni–S distances of 2.21 Å and two Ni–N/O distances of 1.97 Å predicted by EXAFS experiments on the nickel-containing CO dehydrogenase enzyme *Clostridium thermoaceticum*.[17] It is also important to recognize that substitution of Ni(II) for Cu(II) in studies of $Cu^{II}N_2S_2$ biological systems could result in a flattened coordination geometry as compared to the proposed pseudotetrahedral active-site geometry. Although many questions remain concerning coordination details at the active sites of nickel metalloproteins, these three systematically distorted Ni(II) structures offer evidence on the relationship between physical properties and different coordination geometries involving a consistent $[N_2S_2]^{2-}$ ligand donor set.

Acknowledgment. We wish to thank Dr. S. Sankar of the North Carolina State University NMR facility for helpful discussions and invaluable assistance in operating the various NMR spectrometers.

Supplementary Material Available: Tables of crystallographic data, atomic coordinates and isotropic thermal parameters, bond distances and angles, non-hydrogen atom anisotropic thermal parameters, calculated parameters for hydrogen atoms, and structure–property relationships for I–III (23 pages); tables of calculated and observed structure factor amplitudes for I–III (60 pages). Ordering information is given on any current masthead page.

(49) LaMar, G. N.; Horrocks, W. D.; Holm, R. H. *NMR of Paramagnetic Ions*; Academic Press: New York, 1973, pp 243–326.
(50) Holm, R. H. *Acc. Chem. Res.* **1969**, *2*, 307.
(51) Gerlach, D. H.; Holm, R. H. *J. Am. Chem. Soc.* **1969**, *91*, 3457.